

# New approach for synthesis of activated carbon from bamboo

Toshiki Tsubota<sup>1</sup> · Masaki Morita<sup>1</sup> · Sunao Kamimura<sup>1</sup> · Teruhisa Ohno<sup>1</sup>

Published online: 27 October 2015  
© Springer Science+Business Media New York 2015

**Abstract** Unconventional pretreatment, that is, delignification and the addition of guanidine phosphate, was performed for the synthesis of activated carbon having a high specific surface area from bamboo by physical activation. The values of the specific surface area, total pore volume, and average pore size depended on the amount of added guanidine phosphate and the CO<sub>2</sub> activation time. The amount of the added guanidine phosphate under the optimum conditions for the highest specific surface area was much lower than that of the phosphorous acid chemical activator under conventional conditions. The N<sub>2</sub> adsorption isotherms of all the samples were type I, which means that micropores were dominant. The pore sizes of the samples in this study were similar to that of the physically-activated carbon. Therefore, the activation process was presumed to be essentially not chemical, but physical. The relation between the yield and the specific surface area improved with the addition of guanidine phosphate. The reason for the improvement may be the change in the reactivity of the carbon material generated during the heating process. The maximum specific surface area was ca. 2000 m<sup>2</sup> g<sup>-1</sup>, which is a high value for a physically-activated carbon.

**Keywords** Activated carbon · Guanidine phosphate · Physical activation · Delignification · Bamboo

## 1 Introduction

Activated carbon is widely used in various industrial fields, such as an adsorbent [1, 2], electrical double layer capacitor [3–5], etc. Some types of organic compounds, such as fossil fuels [6], synthetic polymers [7], and biomass [8], were used as the raw material for the activated carbon. From the viewpoint of global warming, the use of biomass has an advantage in CO<sub>2</sub> emissions.

There are two types of methods for the activation, that is, physical activation and chemical activation. In the case of physical activation, an oxidized gas, such as H<sub>2</sub>O, CO<sub>2</sub>, and O<sub>2</sub>, was used for the treatment. On the other hand, in the case of chemical activation, a chemical activator, such as KOH, ZnCl<sub>2</sub>, and H<sub>3</sub>PO<sub>4</sub>, was used for the treatment. In general, the specific surface area of the chemically-activated carbon is greater than that of the physically-activated carbon. Moreover, chemical activation has an advantage in the control of the pore size and pore distribution. Especially, KOH is an excellent activator because it can realize a high specific surface area [9]. However, the use of KOH requires attention because metallic potassium, which can be generated during the activation process at a high temperature, is chemically reactive. In general, physical activation is safer than chemical activation, and physical activation can easily produce micropores [10]. Therefore, the preparation method of the physically-activated carbon having a high specific surface area equivalent to chemically-activated carbon is valuable. Some researchers compared the chemical activation and physical activation [11–13], and some researchers attempted to use the combination

---

**Electronic supplementary material** The online version of this article (doi:10.1007/s10934-015-0087-6) contains supplementary material, which is available to authorized users.

---

✉ Toshiki Tsubota  
tsubota@che.kyutech.ac.jp

<sup>1</sup> Department of Applied Chemistry, Faculty of Engineering, Kyushu Institute of Technology, 1-1 Sensuicho, Tobata-ku, Kitakyushu 804-8550, Japan

of a chemical activator and physical activation. Mahboub et al. [14] tried to optimize the combination of chemical activation with  $\text{ZnCl}_2$  and  $\text{CO}_2$  activation. Zhang et al. [15] attempted the combination of KOH activation and  $\text{CO}_2$  activation. The combination of phosphoric acid activation and  $\text{CO}_2$  activation was performed to produce carbon fibers derived from poly(*p*-phenylene benzobisoxazole) [16].

In the field of flame retardants, guanidine phosphate is known to be one of the flame retardants for cellulosic materials. We reported that the addition of guanidine phosphate improved the performance of the carbon material derived from a polysaccharide, such as starch and cellulose, as the electrode of an electrochemical capacitor [17–19]. Moreover, we published a paper describing the  $\text{CO}_2$  activation of guanidine phosphate-added spherical cellulose [20].

In general, plants consist of cellulose, hemicellulose, and lignin. Cellulose and hemicellulose are polysaccharides and lignin is a polymer of aromatic compounds. If lignin is selectively removed while maintaining the microstructure derived from plant tissue, a porous polysaccharide material can be formed. It is known that the carbon material derived from cellulose and hemicellulose is easily activated with a high specific surface area. However, the yield is relatively low because the polysaccharide, such as cellulose, contains a high percentage of oxygen atoms. Therefore, in this study, the combination of delignification, guanidine phosphate, and  $\text{CO}_2$  activation was investigated in detail.

## 2 Experimental

In this study, dried bamboo powder (<0.5 mm in size) was used as the starting material. The delignification process was performed using the mixture of  $\text{CH}_3\text{COOH}$  and  $\text{H}_2\text{O}_2$ . The bamboo (20 g) was added to the mixture of  $\text{CH}_3\text{COOH}$  (Wako Pure Chemical Industries, Ltd., 99 %) (100 mL) and an  $\text{H}_2\text{O}_2$  aqueous solution (Wako Pure Chemical Industries, Ltd., ca. 30 %) (100 mL), then the slurry was heated at 85 °C for 0–8 h. The treated sample was washed with distilled water, then dried in a dryer for more than 1 day. The dried sample was mixed with guanidine phosphate (Wako Pure Chemical Industries, Ltd., 97 %) (0–50 wt% against the dried sample) in water. The slurry was dried in a dryer for more than 1 day. The dried sample was placed in an electric furnace, then heated to 800 °C at the heating rate of ca. 20 °C per minute under flowing  $\text{N}_2$ . The final temperature was maintained for 1 h and then the temperature decreased to room temperature under flowing  $\text{N}_2$ . In the case of activation, the temperature was maintained for 1 h under flowing  $\text{N}_2$ , and then the flowing gas was changed from  $\text{N}_2$  to  $\text{CO}_2$ . The temperature

was maintained for 0–5 h along with the flowing  $\text{CO}_2$ , then the flowing gas was changed from  $\text{CO}_2$  to  $\text{N}_2$  and the temperature decreased to room temperature. The samples after the heat treatment were washed with hot water, then dried in a dryer.

The UV–Vis measurements (UV-2600, SHIMADZU CORPORATION) of the samples after the delignification process was done by diffuse reflection method for the quantitative evaluation of the color change in the samples. The  $\text{N}_2$  adsorption isotherms were then measured (nova4200e, Quantachrome Instruments). The BET method was used for the estimation of the specific surface area of the samples at a relative pressure,  $p/p_0$ , in the range of 0 to <0.1 (the value of the correlation coefficient is >0.9995.) because micropores were dominant in the samples. The pore size distributions, micropore volumes, and total pore volumes were calculated by the DFT method. The average pore sizes were estimated from the data at the highest relative pressure of the  $\text{N}_2$  adsorption isotherm and the values of the specific surface area calculated by the BET method.

## 3 Results and discussion

### 3.1 Delignification process

In order to remove the lignin, the samples were treated with the mixture of  $\text{CH}_3\text{COOH}$  and  $\text{H}_2\text{O}_2$ . The color of the samples was changed by increasing the treatment time. For the estimation of the color change of the sample, the UV–Vis spectra were measured by the diffuse reflection method. The UV–Vis spectra for the samples after the treatment with the mixture of  $\text{CH}_3\text{COOH}$  and  $\text{H}_2\text{O}_2$  are shown in Fig. 1 as a function of the delignification time. The reflectance increased with the increasing reaction time up to 0.75 h, then decreased up to 2 h, and then increased again with the increasing reaction time. The decomposition of the lignin in the bamboo should be the main reason for the change in the reflectance. Although the reason for the local minimum of the reflectance at ca. 2 h was unclear, the generated species derived from the lignin could be the origin of the absorption.

The delignification time dependence of the yield [ $100 \times (\text{weight after the treatment with the mixture of } \text{CH}_3\text{COOH} \text{ and } \text{H}_2\text{O}_2) / (\text{weight before the treatment with the mixture of } \text{CH}_3\text{COOH} \text{ and } \text{H}_2\text{O}_2)$ ] is shown in Fig. 2. Moreover, the yield after the heat treatment at 800 °C for 1 h under flowing  $\text{N}_2$ , that is, the yield [ $100 \times (\text{weight after the heat treatment}) / (\text{weight before the heat treatment})$ ] is also shown in Fig. 2. These yields drastically decreased with the increasing reaction time to 1 h, then these values were almost independent of the delignification time. The

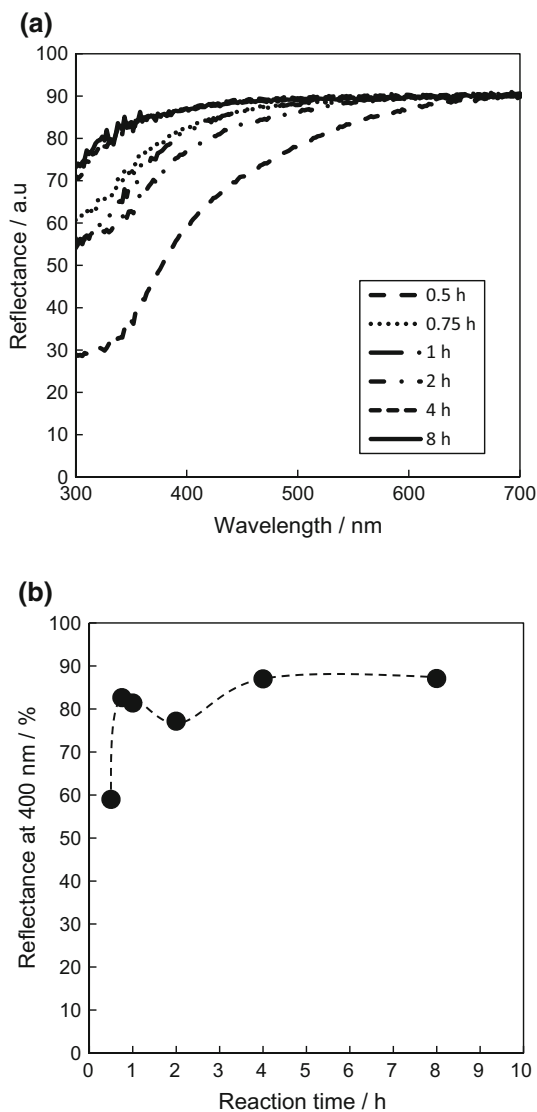


**Fig. 1** The UV–Vis spectra of the samples after the treatment with the mixture of CH<sub>3</sub>COOH and H<sub>2</sub>O<sub>2</sub>

percentages of oxygen in the cellulose and hemicellulose should be greater than that in the lignin because cellulose and hemicellulose are types of polysaccharides, while lignin is known as a polymer of aromatic compounds. Therefore, the yields from the heat treatment of the polysaccharides could be lower than that for lignin. The removal of lignin could be the reason for the decrease in the yield by the heat treatment of the samples. The measured percentage of lignin in the sample after the 8-h delignification process was under the limit of detection (by the Klason method), whereas that for the sample before the process was 23.4 %. Because these yields in Fig. 2 are almost constant when the delignification process was >8 h, the sample treated for 8 h was used as the starting material for the addition of guanidine phosphate and CO<sub>2</sub> activation.

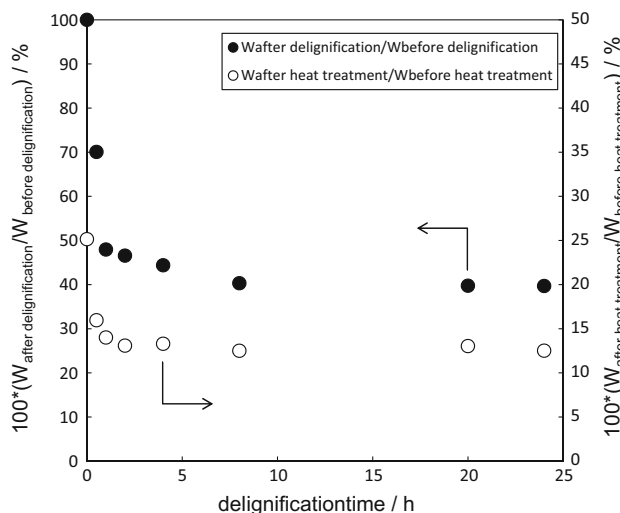


**Fig. 2** Treatment time dependence of the yields

### 3.2 Effect of CO<sub>2</sub> activation

First, the effect of the CO<sub>2</sub> activation was investigated in detail. The amount of guanidine phosphate mixed with the bamboo after the delignification was 4.8 wt%. The N<sub>2</sub> adsorption isotherms of the samples after the heat treatment are shown in Fig. 3a. The graphs of all the samples were type-I, which means that there are micropores in the samples. The sample at “0 h”, that is, after the delignification process with the addition of guanidine phosphate and no CO<sub>2</sub> activation, adsorbed a higher amount of N<sub>2</sub> than the sample derived from bamboo, that is, no delignification treatment and no addition of guanidine phosphate before the heat treatment. The volume of adsorbed N<sub>2</sub> increased with the increasing CO<sub>2</sub> activation time up to 3 h, then decreased with the increasing CO<sub>2</sub> activation time of more than 3 h. The pore size distributions of the samples calculated by the DFT method are shown in Fig. 3b. The calculated pore width increased with the increasing CO<sub>2</sub> activation time.

The average pore sizes and the pore volumes of the samples are shown in Fig. 4a. In the case of no CO<sub>2</sub> activation, the total pore volume and micropore volume were enhanced by the delignification process with the addition of guanidine phosphate although the average pore size was not affected by the treatment. Both the micropore (<2 nm) volume and the volume of the pores other than the micropores (more than 2 nm) increased with the increasing activation time up to 3 h, resulting in the maximum total pore volume at 3 h. The average pore size also reached a maximum at 3 h. Gaseous activation is considered to proceed in two stages. During the first stage, parts of the unorganized structure are selectively decomposed and the closed small pore spaces among the carbon crystalline

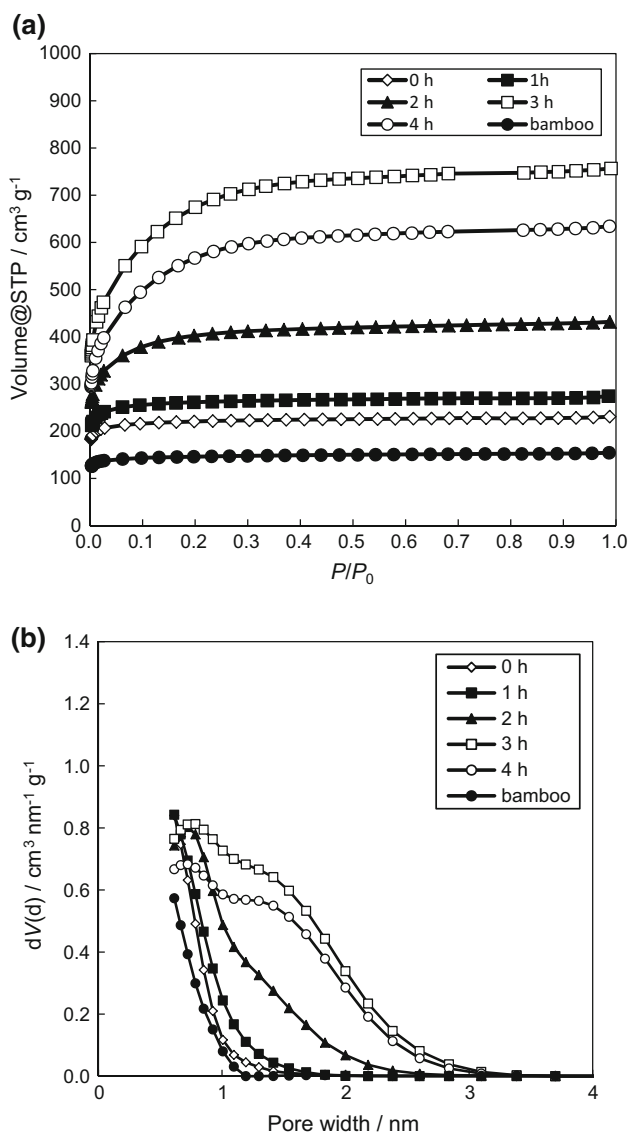


**Fig. 3** Experimental results of N<sub>2</sub> adsorption isotherms. **a** N<sub>2</sub> adsorption isotherms of the samples after the heat treatment, **b** pore size distributions of the samples calculated by DFT method

structure are opened, resulting in a drastically increasing specific surface area. In the second stage, the carbon atoms forming the small pore spaces are decomposed, resulting in the formation of larger sized pores. Based on the experimental results, the effect of the first stage could be significant up to 2 h, and the effect of the second stage could dominate after 3 h.

The BET specific surface areas of the samples are shown in Fig. 4b. In the case of no CO<sub>2</sub> activation, the specific surface area was enhanced by combination of the delignification process and the addition of guanidine phosphate. The specific surface area increased with the increasing CO<sub>2</sub> activation time up to 3 h, and reached ca. 2000 m<sup>2</sup> g<sup>-1</sup>. The reported specific surface areas of the activated carbons,

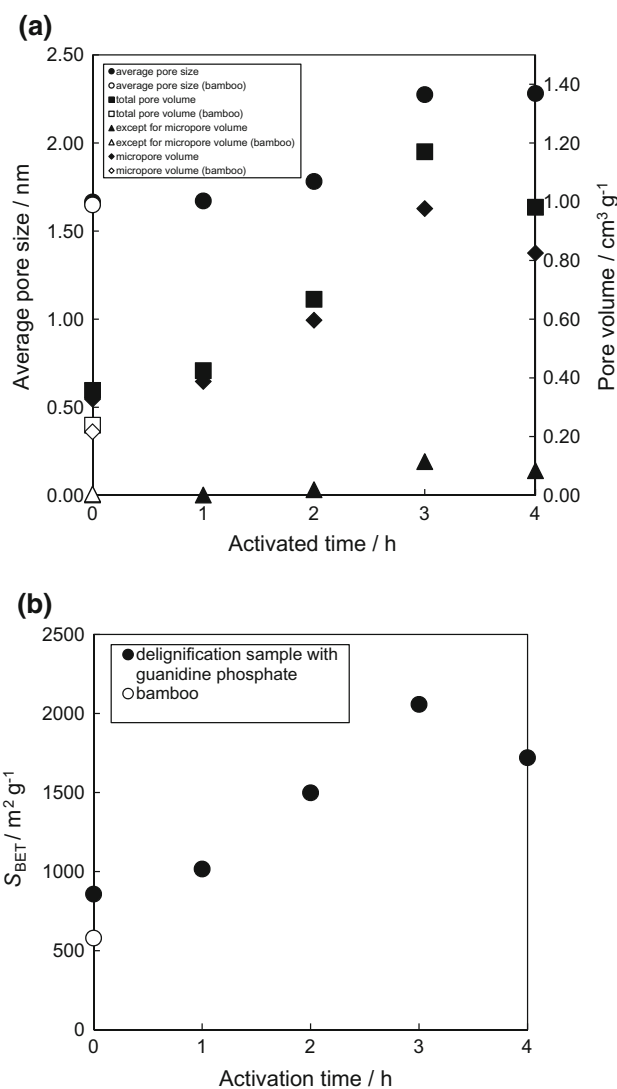


**Fig. 4** Estimated results from N<sub>2</sub> adsorption isotherms. **a** Average pore sizes and the pore volumes of the samples, **b** BET specific surface areas of the samples

which were derived from the biomass and synthesized by the gaseous activation, were ca. 1700 m<sup>2</sup> g<sup>-1</sup> at most [21–23]. In spite of the small amount of the additive, such as guanidine phosphate, the specific surface area obtained in this study is greater than that previously reported for the physically-activated carbon. Sanchez et al. [24] reported that the activated carbon synthesized by the CO<sub>2</sub> activation from cedar wood after H<sub>2</sub>O<sub>2</sub> treatment had a specific surface area of 1705 m<sup>2</sup> g<sup>-1</sup>, and the authors considered that the H<sub>2</sub>O<sub>2</sub> treatment resulted in no removal of the lignin, but oxidation of the surface because the yield of the H<sub>2</sub>O<sub>2</sub> treatment was nearly 100 %. Therefore, although the mechanism in this study is different from that of Sanchez's study, the pretreatment with the H<sub>2</sub>O<sub>2</sub> mixture could be effective for changing the specific surface area (the data of

Fig. 4 are summarized in Table s1 in supporting information).

### 3.3 Effect of guanidine phosphate

Next, the amount of the added guanidine phosphate dependence was investigated in detail. The CO<sub>2</sub> activation time was 3 h. The N<sub>2</sub> adsorption isotherms of the samples are shown in Fig. 5a. All the samples indicated type-I graphs as well as the samples in Fig. 3a, although the flexion at  $P/P_0 = ca. 0.1$  moderated with the change in the added guanidine phosphate. The volume of adsorbed N<sub>2</sub>

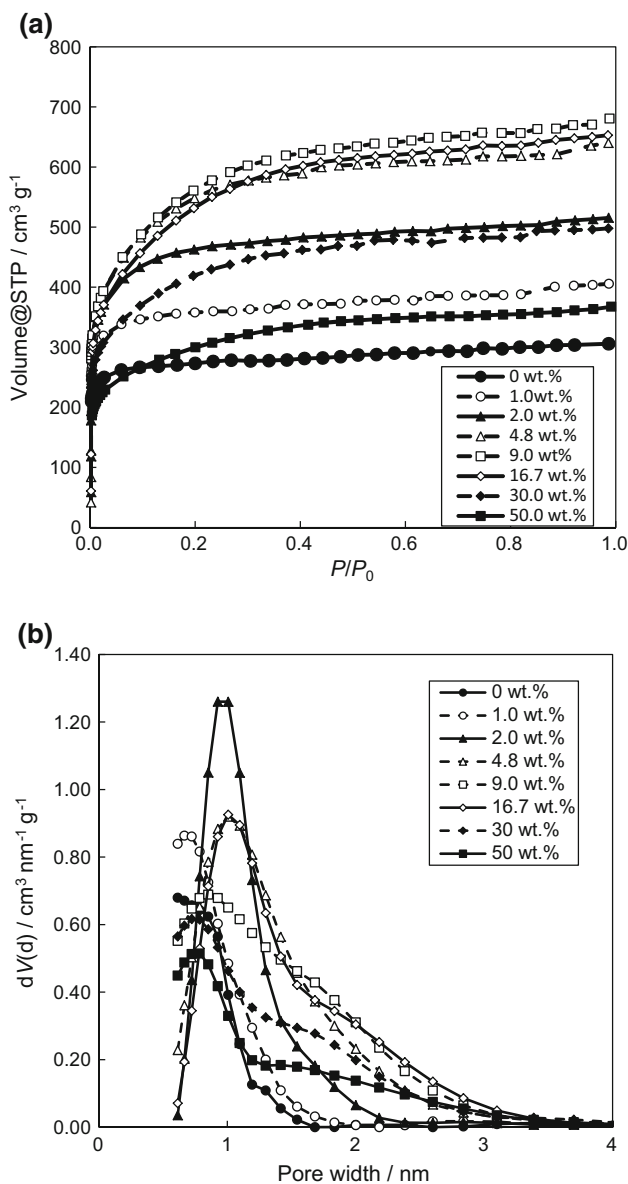


**Fig. 5** Experimental results of N<sub>2</sub> adsorption isotherms. **a** N<sub>2</sub> adsorption isotherms of the samples, **b** pore size distributions of the samples calculated by DFT method

increased with the increasing amount of the added guanidine phosphate up to 9.0 wt%. The pore size distributions of the samples calculated by the DFT method are shown in Fig. 5b. The pore size distribution was affected by the guanidine phosphate addition.

The average pore sizes and the pore volumes are shown in Fig. 6a. The specific surface areas of the samples are shown in Fig. 6b. These values reached maximums at 4.8–9.0 wt%, and the excessive addition of guanidine phosphate resulted in the suppression of these values. For the chemical activation by phosphoric acid, the maximum specific surface area appeared when the amount of the added phosphoric acid was typically 50 wt% or more [25, 26]. Therefore, the chemical activation by phosphoric acid derived from guanidine phosphate could not be the main reason for the activation in this study. The yield, that is,  $100 \times (\text{weight after activation process}) / (\text{weight before activation process})$  increased with increasing the amount of guanidine phosphate. We have already reported that the

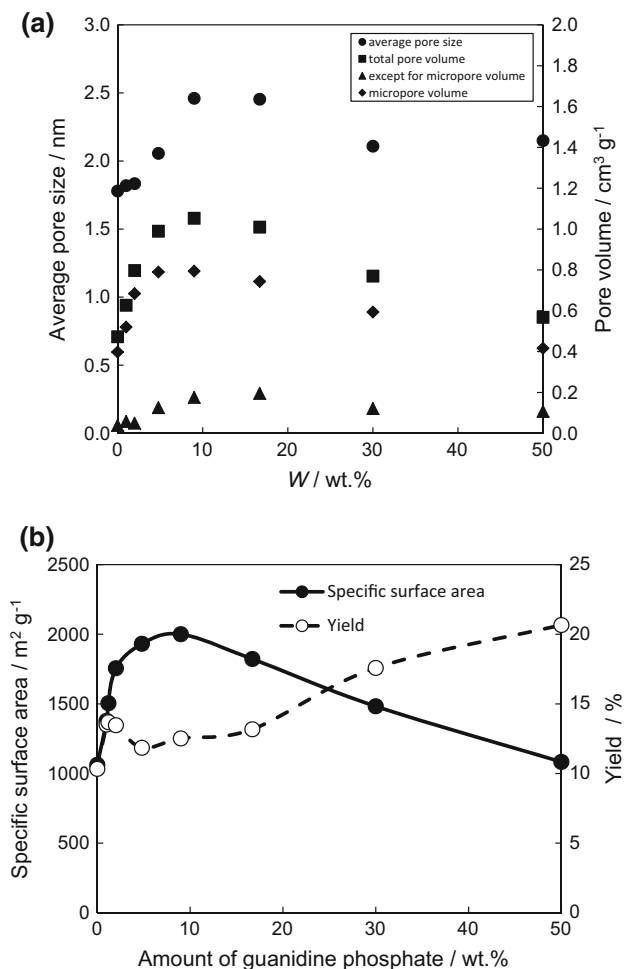


**Fig. 6** Estimated results from N<sub>2</sub> adsorption isotherms. **a** Average pore sizes and the pore volumes of the samples, **b** BET specific surface areas of the samples

addition of guanidine phosphate to cellulose increases the yield [20]. Because the samples after the delignification process mainly consisted of cellulose, the change in the yield is reasonable (the data of Fig. 6 are summarized in Table s2 in supporting information, and the SEM images are shown in Fig. s1 in supporting information).

The percentages of C, H, N, etc., of the samples are listed in Table 1. The percentage of N increased with the increasing amount of the added guanidine phosphate. Moreover, the percentage of the others, which was calculated according to the following formula, “the percentage of others” = 100 – (“the percentage of C” + “the percentage of H” + “the percentage of N”), increased by the addition of guanidine phosphate. Most of “the percentage of others” could consist of O atoms and P atoms. The XPS spectrum assigned to P 2*p* and that assigned to N 1*s* for the 4.8 wt% sample are shown in Fig. 7. The existence of the P atoms on the sample was confirmed by the XPS peak shown in Fig. 7a. Some researchers reported that the activated carbon synthesized using phosphoric acid had P atoms on the surface [27, 28]. It should be presumed that the P atoms on the samples could be derived from the guanidine phosphate. There were several peaks in the XPS spectrum for N 1*s*. The separated peaks existed at 398.3, 400.8, 402.8, and 405.3 eV. Konno et al. [29] tried to assign the N peaks based on the reported data and mentioned that, in general, nitrogen doped carbon had peaks assigned to the pyridinic N, pyrrolic N, quaternary N, and N-oxide. The two peaks in this study could be assigned to the pyridinic N (398.3 eV) and pyrrolic N (400.8 eV) because the peak positions were similar to those of the reported values. Although the positions of the other two peaks differed from those of the reported values, the peaks at 402.8 and 405.3 eV may be assigned to the quaternary N and N-oxide, respectively.

Because the percentage of lignin was almost zero for the sample after the delignification for 8 h, the sample should consist of polysaccharides such as cellulose and hemicellulose. It is known that the pyrolysis of cellulose proceeds in four stages. During stage I, the physisorbed water desorbs from 23 to 150 °C. During stage II, the desorption of water from the cellulose ring occurs from 150 to 240 °C. During stage IIIa, the desorption of water via cleavage of the glycosidic linkage occurs from 240 to 400 °C. During stage IIIb, the generation of CO and CO<sub>2</sub> occurs from 240

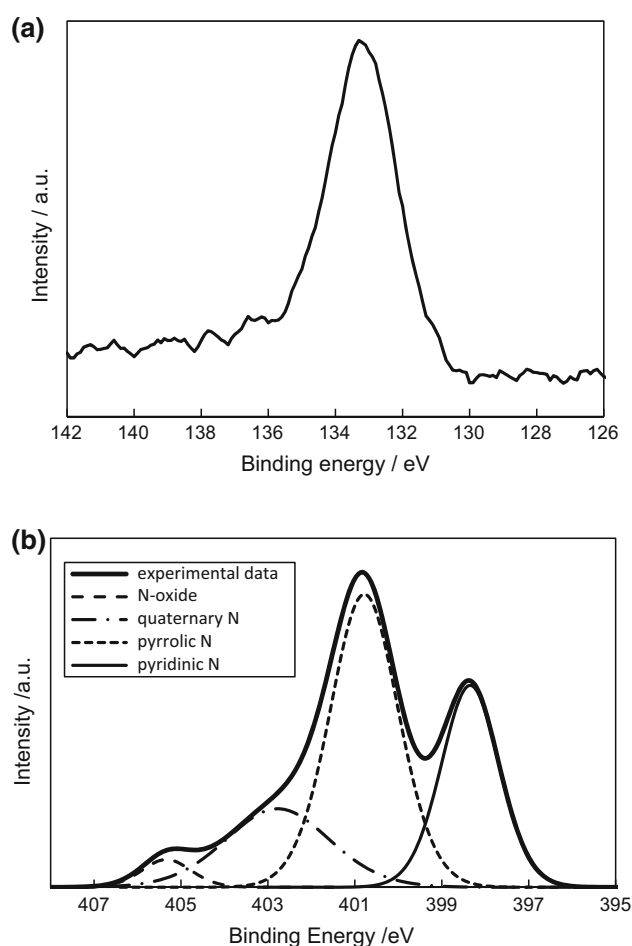


Fig. 7 XPS spectra for the 4.8 wt% sample. a P 2*p*, b N 1*s*

to 400 °C. During stage IV, the generation of H<sub>2</sub> via aromatization occurs from 400 to 700 °C. The phosphorous compounds are presumed to suppress the pyrolysis temperature, resulting in favoring stage II rather than stage III [30]. That is, the phosphorous compound, such as guanidine phosphate, may affect the chemical structure of the synthesized carbon material. This might be the reason for the high specific surface area for the CO<sub>2</sub> activation. Moreover, it is known that a part of the phosphorous is retained in the carbon material and that some of the nitrogen is retained in the carbon material [30]. Therefore, the existence of the phosphorous atoms and the nitrogen atoms in the sample is reasonable.

**Table 1** The percentages of C, H, N, etc., of the samples

Amount of added guanidine phosphate (wt%)	C (wt%)	H (wt%)	N (wt%)	Others (wt%)
0	88.60	1.00	0	10.40
9	75.74	1.27	3.37	19.62
50	66.27	1.84	7.07	24.82

The experimental results are summarized as follows:

1. The combination of delignification, the addition of guanidine phosphate and CO<sub>2</sub> activation is effective for the synthesis of activated carbon having a high specific surface area from bamboo.
2. The obtained specific surface area, ca. 2000 m<sup>2</sup> g<sup>-1</sup>, is very high for the physically-activated carbon, and the amount of the additive is very low for the chemically-activated carbon.
3. The activated carbon synthesized in this study should contain phosphorous atoms and nitrogen atoms.

## 4 Conclusions

The combined treatment of delignification, the addition of guanidine phosphate, and CO<sub>2</sub> activation for bamboo as the starting material was effective for the preparation of an activated carbon having a high specific surface area without using the conventional chemical activator. The specific surface area of the prepared sample in this study reached ca. 2000 m<sup>2</sup> g<sup>-1</sup>, which is a very high value for the physically-activated carbon. The guanidine phosphate should interact with the cellulose during the heating process, resulting in the introduction of the nitrogen and phosphorous atoms in the carbon material.

**Acknowledgments** The dried bamboo powder used in this study was provided by Bamboo Chemical Laboratory Co., Ltd. The authors express our thanks to Masayuki Tsuruha, a representative of the Bamboo Chemical Laboratory Co., Ltd. The authors thank Prof. Yukie Saito of the Graduate School of Agricultural and Life Sciences, The University of Tokyo, for her advice about the delignification method. This work was supported by JSPS KAKENHI Grant No. 26410253 and the Yamagin regional enterprise support foundation.

## References

1. A. Bhatnagar, W. Hogland, M. Marques, M. Sillanpaa, *Chem. Eng. J.* **219**, 499 (2013)
2. J. Rivera-Utrilla, M. Sanchez-Polo, V. Gomez-Serrano, P.M. Alvarez, M.C.M. Alvim-Ferraz, J.M. Dias, *J. Hazard. Mater.* **187**, 1 (2011)
3. D. Qu, H. Shi, *J. Power Source* **74**, 99 (1998)
4. O. Barbieri, M. Hahn, A. Herzog, R. Kotz, *Carbon* **43**, 1303 (2005)
5. H. Shi, *Electrochim. Acta* **41**, 1633 (1996)
6. C. Moreno-Castilla, J. Rivera-Utrilla, M.V. Lopez-Ramon, F. Carrasco-Marin, *Carbon* **33**, 845 (1995)
7. S. Villar-Rodil, F. Suarez-Garcia, J.I. Paredes, A. Martinez-Alonso, J.M.D. Tascon, *Chem. Mater.* **17**, 5893 (2005)
8. O. Ioannidou, A. Zabaniotou, *Renew. Sustain. Energy Rev.* **11**, 1966 (2007)
9. M.J. Illan-Gomez, A. Garcia-Garcia, C.S.M. Lecea, A. Linares-Solano, *Energy Fuel* **10**, 1108 (1996)
10. A. Aworn, P. Thiravetyan, W. Nakbanpote, *J. Anal. Appl. Pyrolysis* **82**, 279 (2008)
11. C. Moreno-Castilla, F. Carrasco-Marin, M.V. Lopez-Ramon, M.A. Alvarez-Merino, *Carbon* **39**, 1415 (2001)
12. M. Ruiz-Fernandez, M. Alexandre-Franco, C. Fernandez-Gonzalez, V. Gomez-Serrano, *Adsorption* **17**, 621 (2011)
13. M.J. Prauchner, F. Rodriguez-Reinoso, *Micropor. Mesopor. Mater.* **152**, 163 (2012)
14. M.J.D. Mahboub, A. Ahmadpour, H. Rashidi, N. Jahanshahi, *Adsorption* **18**, 297 (2012)
15. Z.A. Zhang, M. Cui, Y.Q. Lai, J. Li, Y.X. Liu, *J. Cent. South Univ. Technol.* **16**, 91 (2009)
16. M.B. Vazquez-Santos, A. Martinez-Alonso, J.M.D. Tascon, *J. Anal. Appl. Pyrol.* **95**, 68 (2012)
17. T. Tsubota, Y. Miyauchi, N. Murakami, T. Ohno, *J. Power Sources* **196**, 5769 (2011)
18. T. Tsubota, T. Yamaguchi, C.S. Wang, Y. Miyauchi, N. Murakami, T. Ohno, *J. Power Sources* **227**, 24 (2013)
19. T. Tsubota, C.S. Wang, N. Murakami, T. Ohno, *J. Power Sources* **225**, 150 (2013)
20. T. Tsubota, D. Nagata, N. Murakami, T. Ohno, *J. Appl. Polym. Sci.* **131**, 40950 (2014)
21. P. Paraskeva, D. Kalderis, E. Diamadopoulos, *J. Chem. Technol. Biotechnol.* **83**, 581 (2008)
22. A.C. Lua, J. Guo, *Carbon* **38**, 1089 (2000)
23. S. Guo, J. Peng, W. Li, K. Yang, L. Zhang, S. Zhang, H. Xia, *Appl. Surf. Sci.* **255**, 8443 (2009)
24. M.L.L. Sanchez, A. Macias-Garcia, M.A. Diaz-Diez, E.M. Cuerda-Correa, J. Ganan-Gomez, A. Nadal-Gisbert, *Appl. Surf. Sci.* **252**, 5984 (2006)
25. X. Wang, D. Li, W. Li, J. Peng, H. Xia, L. Zhang, S. Guo, G. Chen, *BioResources* **8**, 6184 (2013)
26. M. Benadjemia, L. Milliere, L. Reinert, N. Benderdouche, L. Duclaux, *Fuel Process. Technol.* **92**, 1203 (2011)
27. A.M. Puziya, O.I. Poddubnaya, R.P. Socha, J. Gurgul, M. Wisniewski, *Carbon* **46**, 2113 (2008)
28. Y. Sun, Q. Yue, B. Gao, Y. Wang, Y. Gao, Q. Li, *Powder Technol.* **249**, 54 (2013)
29. H. Konno, T. Ito, M. Ushiro, K. Fushimi, K. Azumi, *J. Power Sources* **195**, 1739 (2010)
30. A. Granzow, *Accounts Chem. Res.* **11**, 177 (1978)